Electroplating of zinc and tin alloys with nickel and cobalt from ammonium oxalate electrolytes*

K. A. Kamysheva, R. F. Shekhanov, S. N. Gridchin, and A. V. Balmasov*

Ivanovo State University of Chemistry and Technology,
7 Sheremetevsky prosp., 153000 Ivanovo, Russian Federation.
E-mail: ruslanfelix@yandex.ru

A possibility of preparing good quality electrolytic alloys zinc-nickel, zinc-cobalt, tin-nickel, and tin-cobalt from ammonium oxalate electrolytes of various compositions was shown. The alloy coatings of high quality can be obtained at the current density range from 1 to 3 A dm^{-2}. The introduction into the electrolyte of ammonium oxalate capable of forming stable complexes with Zn^{2+}, Sn^{2+}, Ni^{2+}, and Co^{2+} ions makes it possible to increase the working pH range. Electroplating occurs with high cathodic polarization favoring the formation of qualitative finely crystalline coatings of the plated alloys.

Key words: electrolytic alloys, polarization experiments, protective coatings, electroplating, corrosion resistance.

Galvanized zinc, cadmium, or tin coatings are traditionally used to protect black metals from corrosion. The introduction of the iron subgroup metals (iron, cobalt, and nickel) into the composition of anticorrosion coatings makes it possible to substantially elongate their protective period, because the corresponding binary alloys are characterized by a higher corrosion resistance than the indicated individual metals.[1] The use of compounds forming soluble complexes with ions of the plating metals is a promising trend for the development of new compositions of electrolytes for the electroplating of metals and alloys.[2—18] One of the most efficient complexing components of the electrolyte is ammonium oxalate, whose advantage is the possibility of decomposing the formed complexes in wastewater. We earlier demonstrated the efficiency of application of ammonium oxalate for the stabilization of the electrolyte when manufacturing electrolytic coatings by the iron subgroup metals.[14—17] The purpose of this work is to study electroplating of zinc-nickel, zinc-cobalt, tin-nickel, and tin-cobalt alloys from the ammonium oxalate electrolytes.

Experimental

Solutions of electrolytes were prepared from the analytical purity grade reagents. Each component of the electrolyte was dissolved in distilled water in a separate vessel, each solution was filtered, and the filtered solutions were combined in a common vessel. The acidity of the solution was corrected by the addition of a 25 or a 50% aqueous solution of sulfuric acid. The coatings were plated with an MPS-3005L-3 Matrix laboratory current source on the preliminarily prepared (degreased and activated) samples of the 08kp steel. Electroplating was carried out at 20—50 °C and a cathodic current density of 1—3 A dm^{-2}. The quality of the coatings was determined from the appearance and adhesion with the base metal according to GOST 9.301-86 and GOST 9.302-88, respectively. The surface morphology and compositions of the alloys were studied on a Tescan Vega 3 SBH scanning electron microscope with an elemental analysis accessory. Potentiodynamic cathodic polarization curves were recorded with a P-30J potentiostat at 50 °C at a potential sweep rate of 5 mV s^{-1}. An EVL-1M1 saturated silver chloride electrode served as a reference electrode, and a platinum wire was an auxiliary electrode. The obtained potential values were recalculated relative to the potential of the standard hydrogen electrode (SHE). An I-160MP ionomer was used for measuring pH values. The current efficiency was calculated by the known procedure.[19] The microhardness of the coatings was determined on a PMT-3 instrument according to GOST 9450-76. The roughness of the coating surface was determined using a 170622 model profile meter (LLC Kalibr, Russia). The corrosion tests of the prepared samples were carried out in a 3% solution of NaCl at 25 °C for 20 min. The corrosion diagrams for the zinc-nickel, zinc-cobalt, tin-nickel, and tin-cobalt alloys were constructed using the Rozenfeld′s method.[20] The Rozenfeld′s method included the construction of the cathodic polarization curves on which the potential of the base metal—plating metal system was put, and the corrosion current was determined from this potential. The protection ability of the coatings was also determined by tests of the samples in a salt spray chamber (Weiss SC 450, Germany). The salt solution was 5% NaCl (pH 6.5—7.2), which was sprayed inside the chamber with the tested samples as a mist. The chamber operated for 144 h in the cyclic mode: the salt solution was sprayed for 15 min, kept for 45 min in the switched off chamber

* Based on the materials of the XXI Mendeleev Congress on General and Applied Chemistry (September 9—13, 2019, St. Petersburg, Russia).

Published in Russian in *Izvestiya Akademii Nauk. Seriya Khimicheskaya,* No. 7, pp. 1272—1278, July, 2020.

(one cycle), and then the cycle was repeated. The tests were carried out at 35 °C and a moisture content of 95—100%.

Results and Discussion

The fractional metal distribution diagrams in the Zn^{2+}—Co^{2+}—$C_2O_4^{2-}$—NH_3 and Sn^{2+}—Ni^{2+}—$C_2O_4^{2-}$—NH_3 systems at 25 °C are presented in Fig. 1. The calculation of the ion equilibria by the Brinkley algorithm[21] using the RRSU program[22] shows that the behavior of these systems is mainly determined by the complexation of $C_2O_4^{2-}$ ions with Zn^{2+} and Ni^{2+} ions, and the soluble bis- and tris-complexes are the predominate species in a wide pH range. The formation of stable oxalate and ammonia complexes prevents the formation of the corresponding hydroxides characterized by a low solubility (solubility product (SP) is $7.1 \cdot 10^{-18}$, $6.3 \cdot 10^{-18}$, $2.0 \cdot 10^{-16}$, and $6.3 \cdot 10^{-27}$ for $Zn(OH)_2$, $Ni(OH)_2$ (after aging), $Co(OH)_2$ (after aging), and $Sn(OH)_2$, respectively[23]). This is very important, because the discharge of hydrogen ions occurs along with the metal ion discharge during electroplating of the iron subgroup metals due to a high cathodic polarization, and the concentration of hydroxyl ions noticeably increases in the near-cathodic layer, which can result in the precipitation of the corresponding metal hydroxides.

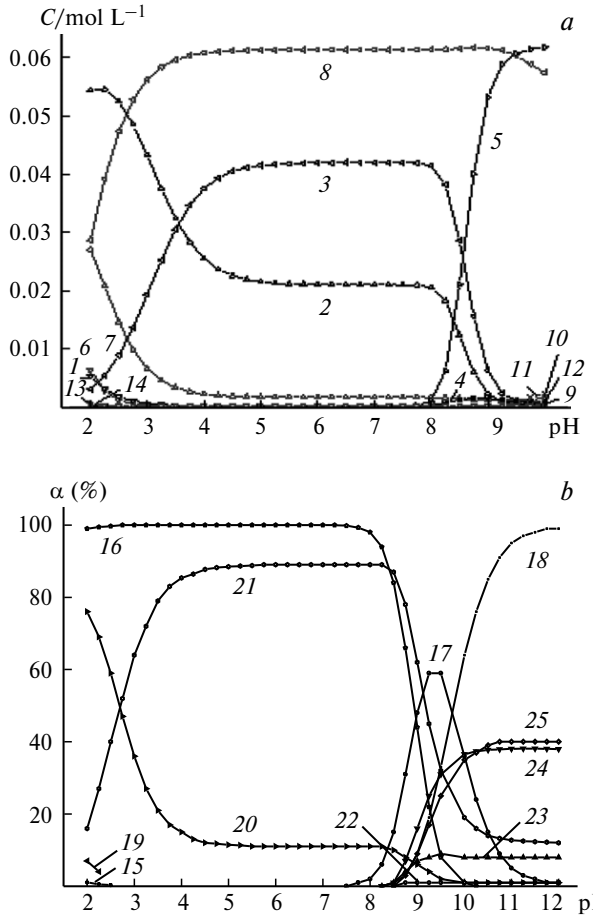

Fig. 1. Diagram of fractional distribution of metals in the Zn^{2+}—Co^{2+}—$C_2O_4^{2-}$—NH_3 (*a*) and Sn^{2+}—Ni^{2+}—$C_2O_4^{2-}$—NH_3 systems (*b*): ZnC_2O_4 (*1*), $Zn(C_2O_4)_2^{2-}$ (*2*), $Zn(C_2O_4)_3^{4-}$ (*3*), $Zn(NH_3)_3^{2+}$ (*4*), $Zn(NH_3)_4^{2+}$ (*5*), CoC_2O_4 (*6*), $Co(C_2O_4)_2^{2-}$ (*7*), $Co(C_2O_4)_3^{4-}$ (*8*), $Co(NH_3)_3^{2+}$ (*9*), $Co(NH_3)_4^{2+}$ (*10*), $Co(NH_3)_5^{2+}$ (*11*), $Co(NH_3)_6^{2+}$ (*12*), $CoSO_4$ (*13*), Co^{2+} (*14*), SnC_2O_4 (*15*), $Sn(C_2O_4)_2^{2-}$ (*16*), $Sn(OH)_2$ (*17*), $Sn(OH)_3^-$ (*18*), NiC_2O_4 (*19*), $Ni(C_2O_4)_2^{2-}$ (*20*), $Ni(C_2O_4)_3^{4-}$ (*21*), $Ni(NH_3)_3^{2+}$ (*22*), $Ni(NH_3)_4^{2+}$ (*23*), $Ni(NH_3)_5^{2+}$ (*24*), and $Ni(NH_3)_6^{2+}$ (*25*). *C* is the equilibrium concentration, and α is the distribution of the corresponding metal (Ni, Sn) over equilibrium forms.

The electroplating of the zinc-nickel alloy from the ammonium oxalate electrolytes (Table 1) occurs with a high cathodic polarization (Fig. 2) favoring the formation of qualitative fine crystalline coatings. The study of the kinetics of the electrochemical processes by cyclic voltammetry (Fig. 3) shows that the discharge of zinc ions occurs at the cathode least difficultly at room temperature, whereas the discharge of nickel ions is characterized by the highest polarization. Three pronounced peaks are observed on the anodic branches of the dependences obtained in electrolytes **A1—A3**. It can be assumed that the first peak corresponds to the dissolution of zinc, the second peak is assigned to alloy dissolution, and the third peak corresponds to the dissolution of nickel. This is confirmed by the cyclic voltammetric curves obtained in the electrolytes containing only nickel or zinc ions. As can be seen from Fig. 3, only one peak corresponding to the anodic oxidation of nickel in a potential range of 300—400 mV is observed on the anodic branch of the curve obtained in electrolyte **A4**, whereas in electrolyte **A5** the single peak corresponding to zinc dissolution is observed at a potential of ~300 mV.

The peaks observed in electrolytes **A1—A3** in the potential range from −300 to +100 mV correspond to the

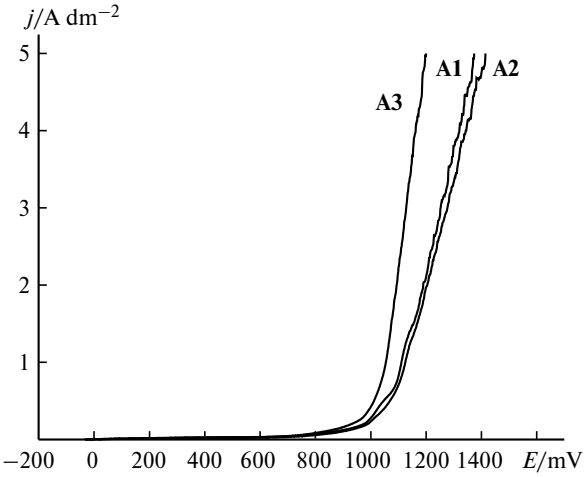

Fig. 2. Cathodic polarization curves for the electroplating of the zinc-nickel alloys from electrolytes **A1—A3** at 50 °C. The potential values *E* are indicated *vs* standard hydrogen electrode.

Table 1. Composition of electrolytes **A1—A5** and properties of the zinc-nickel alloys plated from them*

Electrolyte	Composition of electrolyte/g L^{-1}			Properties of alloy		
	$(NH_4)_2C_2O_4 \cdot H_2O$	$NiSO_4 \cdot 7H_2O$	$ZnSO_4 \cdot 7H_2O$	C_{Ni} (at.%)	H_μ/Pa	j_{corr}/mA cm^{-2}
A1	100	12	24	3.5±0.5	6290	0.27
A2	100	18	18	12.5±0.4	8300	0.22
A3	100	24	12	15.3±0.4	11200	0.19
A4	100	18	0	100	—	—
A5	100	0	18	0	—	—

Note: C_{Ni} is the nickel content in the alloy, H_μ is the microhardness, and j_{corr} is the corrosion current density.
* Conditions: cathodic current density 1 A dm^{-2}, pH 5.6—6.8, 20—50 °C.

dissolution of intermetallic compounds NiZn and Ni_5Zn_{21}, whose formation was found by us earlier by X-ray diffraction analysis.[24] Depending on the ratio of concentrations of discharged metal ions in the composition of the electrolytes indicated in Table 1 and the electroplating conditions, the Zn-Ni alloys contain from 3 to 16 at.% Ni, the rest is zinc, as well as about 1.5 at.% carbon.[15]

Nickel alloying of the zinc coatings results in a substantial change in their physicochemical properties. The microhardness of the coatings increases with an increase in the nickel content in the alloy. The finely crystalline zinc-nickel alloys containing 15—16 at.% Ni are characterized by the highest microhardness compared to other obtained zinc-nickel coatings.

The potential of the coating shifts to the range of more positive values with an increase in the nickel or cobalt content in the coating (see Tables 1 and 2). This results in a decrease in the electromotive force (EMF) of the corrosion cell and a decrease in the corrosion current (Fig. 4). A white film is formed on the sample surface (Fig. 5) in the case of low nickel and cobalt alloying of the zinc alloys when the samples were maintained in the salt spray chamber for 144 h (salt spray, 5% NaCl, 35 °C). The fraction

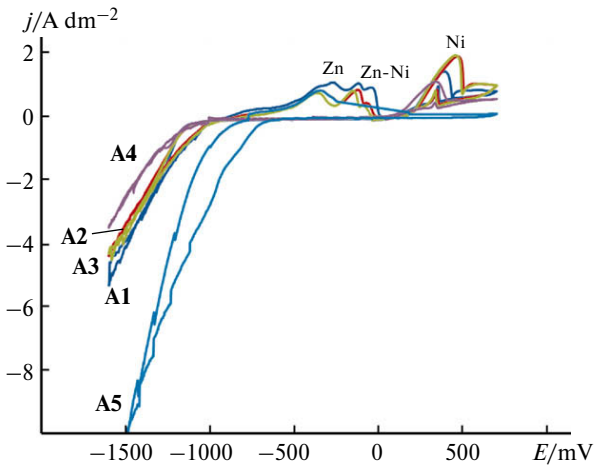

Fig. 3. Cyclic voltammograms obtained in electrolytes **A1—A5** at 20 °C. The potential values E are indicated *vs* standard hydrogen electrode.
Note. Figures 3 and 5 are available in full color on the web page of the journal (https://link.springer.com/journal/volumesAndIssues/11172).

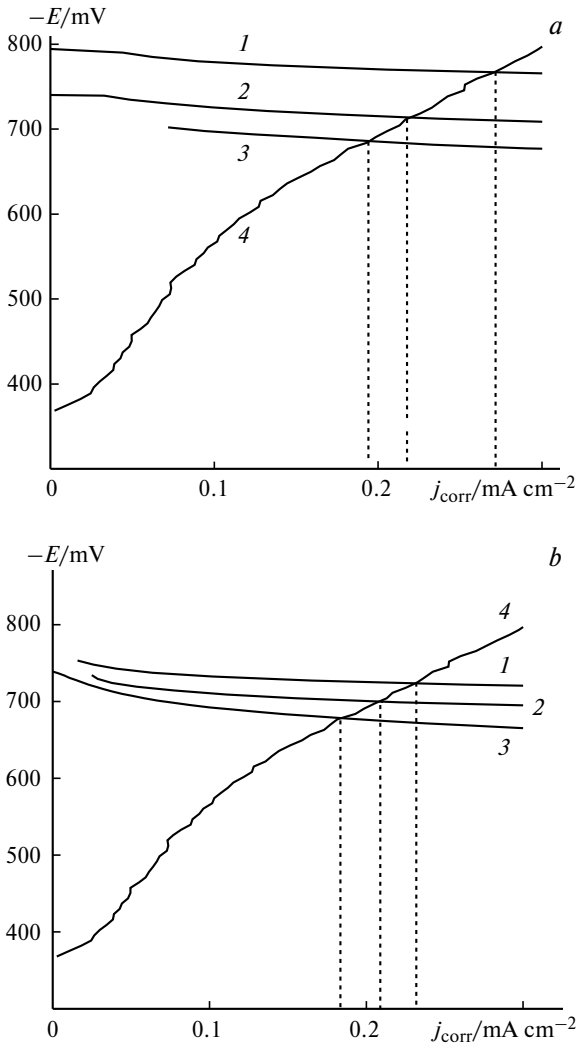

Fig. 4. Corrosion diagrams of the samples of the zinc-nickel (*a*) and zinc-cobalt (*b*) alloys plated from the oxalate electrolytes: *1—3*, anodic curves of the alloys plated from electrolytes **A1—A3** (*a*) and **B1—B3** (*b*); and *4*, cathodic curve at the steel electrode. Conditions for the corrosion tests: 3% NaCl, 25 °C, 20 min.

Table 2. Composition of electrolytes **B1—B3** and properties of the plated zinc-cobalt alloys*

Electrolyte	Composition of electrolyte/g L^{-1}			Properties of alloy		
	$(NH_4)_2C_2O_4 \cdot H_2O$	$CoSO_4 \cdot 7H_2O$	$ZnSO_4 \cdot 7H_2O$	C_{Co} (at.%)	H_μ/Pa	j_{corr}/mA cm^{-2}
B1	100	12	24	3.8±0.2	4145	0.23
B2	100	18	18	8.0±0.4	4214	0.21
B3	100	24	12	12.0±0.5	4381	0.18

Note: C_{Co} is the cobalt content in the alloy, H_μ is the microhardness, and j_{corr} is the corrosion current density.
* Conditions: cathodic current density 1 A dm^{-2}, pH 6.1, 40—50 °C.

of the surface covered with the white film decreases from 60 to 40% on going from the tin-nickel to tin-cobalt alloys. No corrosion of the base metal (08kp steel) on which the coating was plated was observed within the indicated time period for the obtained Zn-Ni and Zn-Co alloys. The amount of the white film on the sample surface was lower for higher alloying of the zinc alloys by nickel and cobalt and especially in the case of highly alloyed coatings. Corrosion damages were observed only near the surface of the stem of the steel sample, which was not protected by the coating. A comparison of the corrosion behavior of the zinc-nickel and zinc-cobalt coatings allows one to

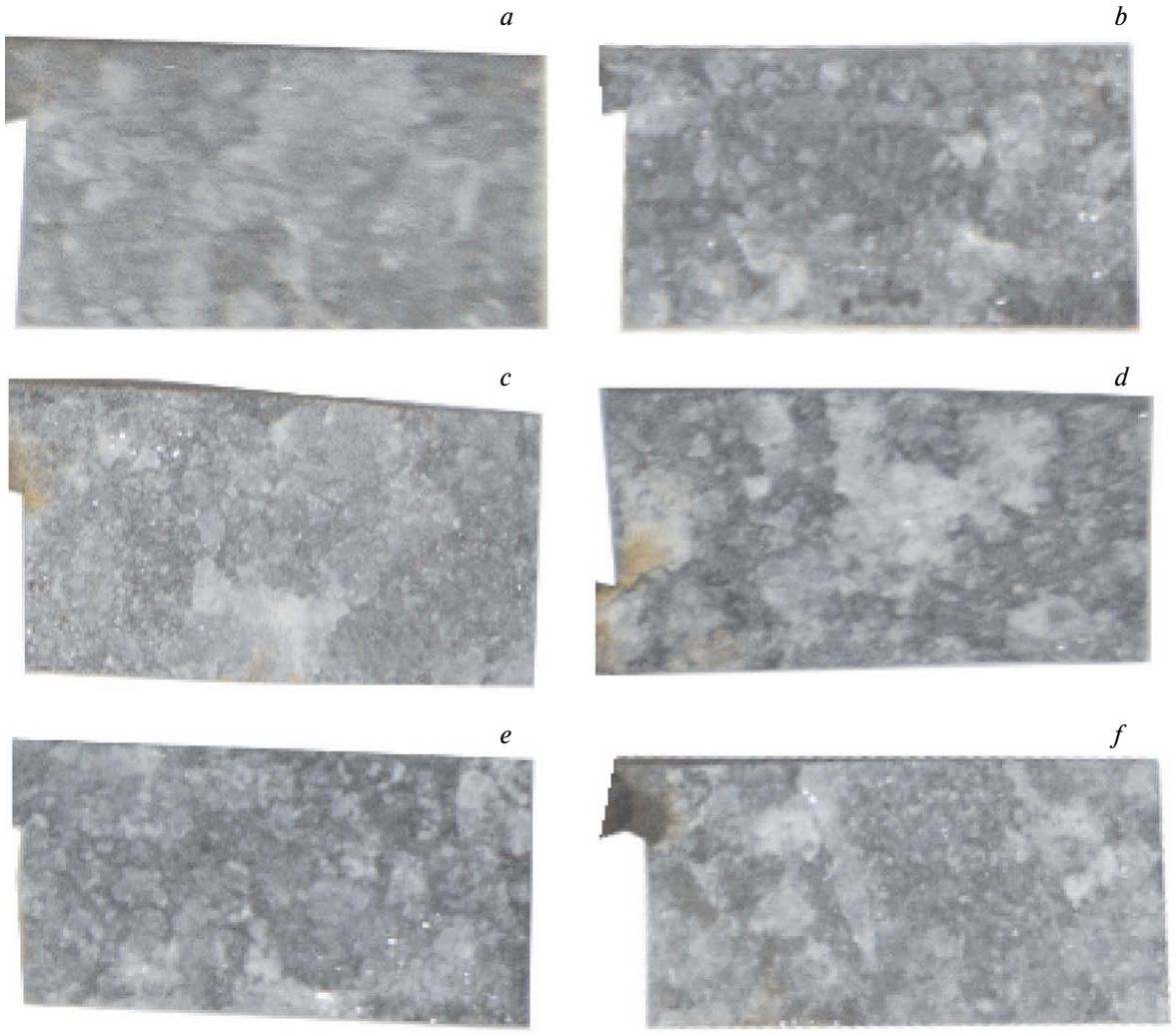

Fig. 5. Images of the samples (1×2 cm) of the zinc-nickel (*a—c*) and zinc-cobalt (*d—f*) coatings plated from ammonium oxalate electrolytes **A1** (*a*), **A2** (*b*), **A3** (*c*), **B1** (*d*), **B2** (*e*), and **B3** (*f*) after corrosion tests in a salt spray chamber (salt spray atmosphere, 5% NaCl, 35 °C, 144 h).

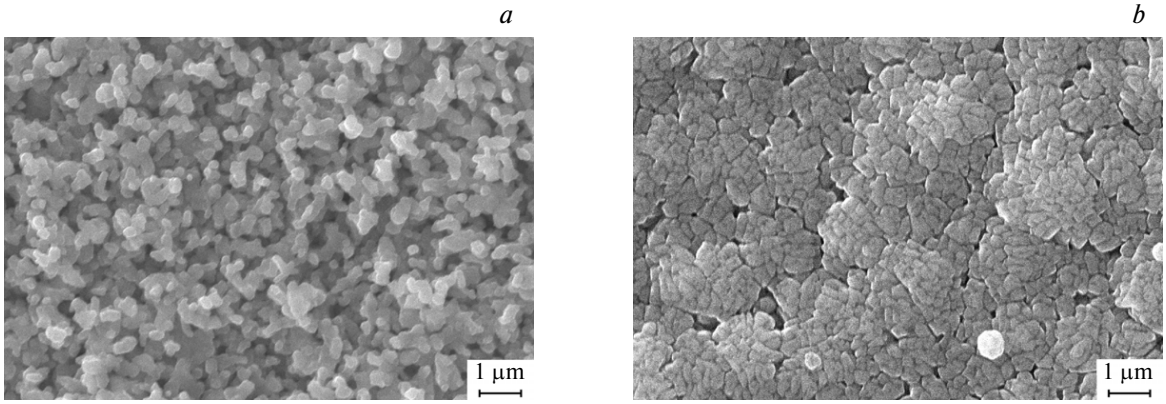

Fig. 6. SEM images of the Zn-Co alloys plated from electrolytes **B1** (*a*) and **B3** (*b*).

conclude that the zinc-cobalt alloys protect against corrosion better than the zinc-nickel coatings. Probably, the higher protective properties of the zinc-cobalt coatings can be explained by somewhat lower EMF between the zinc-cobalt coatings and steel (see Fig. 4) compared to zinc-nickel coatings and also by a special closely packed petal structure of the zinc-cobalt alloys (Fig. 6).

The compositions of the electrolytes used for the plating of the tin-nickel and tin-cobalt alloys are presented in Table 3 together with the mechanical and corrosion characteristics of the plated coatings. The electrolytes studied are distinguished by a high polarizability in the working range of current densities from 0.5 to 3.0 A dm^{-2}, which favors (along with the high polarization) the formation of finely crystalline tin-nickel and tin-cobalt alloys. The maximum slope of the polarization curves obtained in the oxalate electrolytes corresponds to the range of cathodic current density equal to 0.1—1.0 A dm^{-2}. The slope of the curves somewhat decreases with the further increase in the current density. The aforementioned polarization characteristics of the oxalate electrolytes with an additive of synthanol OS-20 (trade mark A) facilitates the approach of the tin and nickel potentials and formation of qualitative fine crystalline bright coatings without using special brightener additives. The use of ammonium oxalate solutions for the electroplating of the Sn-Ni and Sn-Co coatings also leads to an increase in the microhardness and corrosion resistance of the plated coatings due to a significant decrease in the number of pores in the structure of the electrolytic alloy. In addition, the studied ammonium oxalate electrolytes are characterized by a high scattering ability (up to 37.2%), which makes it possible to plate protective coatings on the profile composite units.

The pattern of the voltammetric dependences of tin and cobalt reduction changes with an increase in the cobalt content in electrolytes **C1**—**C4**. Alloy electroplating occurs at more negative potentials, which is due to the retardation of the reduction of the tin and cobalt oxalate complexes. The rate of cathodic potential increasing with an increase in the current density in the ammonium oxalate electrolytes increases with an increase in the cobalt content in the solution (Fig. 7), which favors the alignment of the coating thickness over the whole cathode surface. The study of the microstructure surface of the tin-cobalt alloys showed that the Sn-Co coating obtained using ammonium oxalate electrolyte **C3** had a fine crystalline structure with

Table 3. Composition of electrolytes **C1—C8** and properties of the plated tin-cobalt and tin-nickel alloys

Electrolyte	Composition of electrolyte/g L^{-1}				Properties of alloy	
	$(NH_4)_2C_2O_4 \cdot H_2O$	$SnSO_4$	$CoSO_4 \cdot 7H_2O$	$NiSO_4 \cdot 7H_2O$	R_a/μm	j_{corr}/mA cm^{-2}
C1	80	20	10	0	0.456	0.79
C2	80	10	10	0	0.316	0.18
C3	80	10	20	0	0.434	0.03
C4	80	10	15	0	0.513	0.10
C5	80	10	0	20	0.400	0.02
C6	80	3	0	30	0.410	0.02
C7	80	2	0	40	0.580	0.01
C8*	80	1	0	30	1.860	0.01

Note: R_a is the arithmetic average roughness height, and j_{corr} is the corrosion current density.
* Contained 0.7 g L^{-1} of synthanol OS-20 ($C_{18}H_{37}O(CH_2CH_2O)_{20}H$).

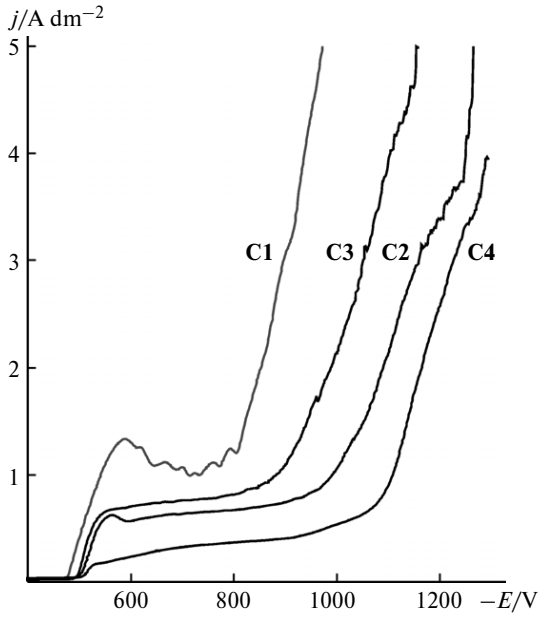

Fig. 7. Overall polarization curves of the Sn-Co coating electroplating and hydrogen evolution at 50 °C for electrolytes **C1—C4**. The potential values *E* are indicated *vs* standard hydrogen electrode.

the grain size 0.5—1 μm, whereas the grain size is 2—4 μm in the case of the cobalt low- and high-alloyed coatings (Fig. 8).

The adhesion strength of the alloy coatings plated from the studied electrolytes to the steel base satisfies the requirements of GOST 9.302-88. No sag of the coatings was observed during tests performed by ploying a network of scratches on the samples with the plated coatings and by the bend method.

Thus, the electroplating of the zinc-nickel, zinc-cobalt, tin-nickel, and tin-cobalt alloys showed that qualitative plates of the alloys can be prepared from the ammonium oxalate electrolytes in the current density range from 1 to 3 A dm^{-2}. The coatings plated from these electrolytes are uniform and characterized by high adhesion to the base metal. Under the same electrolysis conditions, the structures of the crystalline lattices of the alloys depend significantly on the concentration. The ratio of the components in the electrolyte affects the complexation processes and rate of the parallel electrochemical reduction of zinc and tin with the iron subgroup metals. The introduction of chelating ligands into the electrolytes favors a decrease in the corrosion rate of the Zn-Ni and Zn-Co coatings

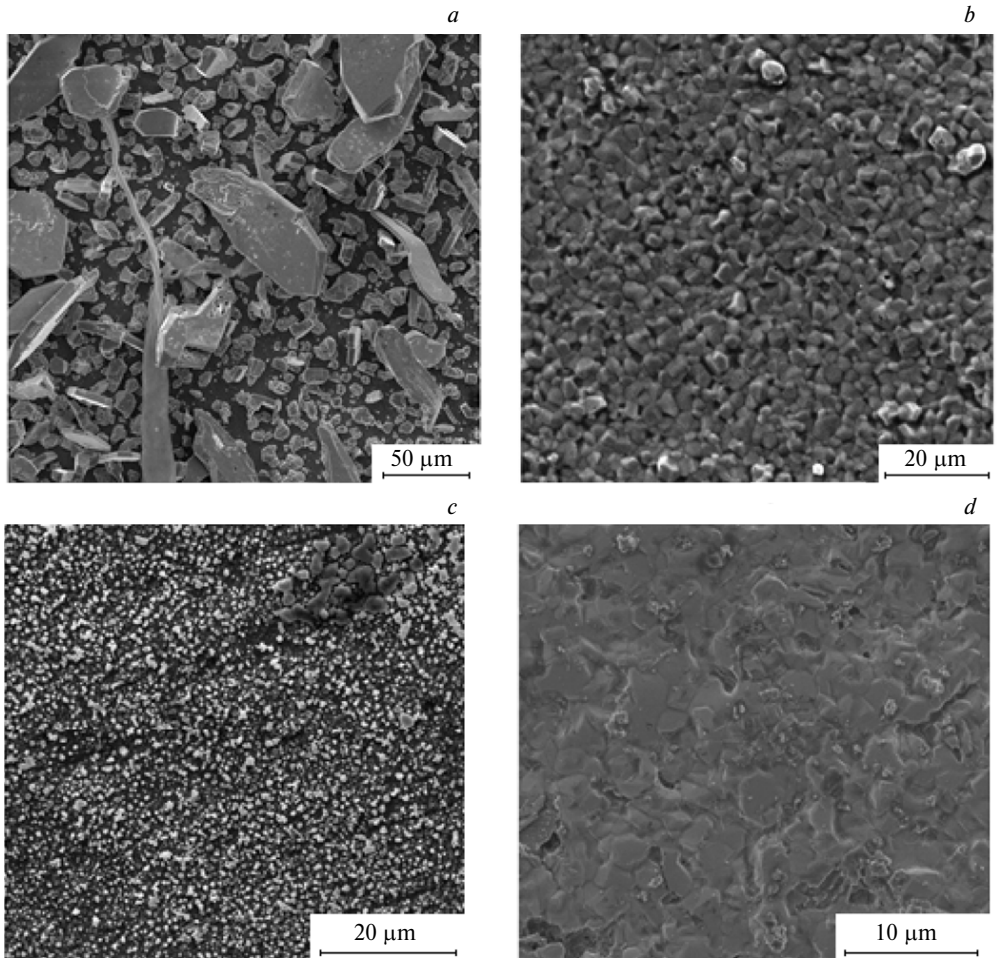

Fig. 8. SEM images of the surface of the Sn-Co coatings plated from electrolytes **C1** (*a*), **C2** (*b*), **C3** (*c*), and **C4** (*d*).

with the retention of the anodic character of steel protection and a decrease in environmental load on wastewater treatment due to a decrease in the toxicity and concentration of the components. The use of ammonium oxalate solutions for the electroplating of the Sn-Ni and Sn-Co coatings also leads to an increase in the microhardness and corrosion resistance of these coatings due to a significant decrease in the number of pores in the plated alloy structure. In addition, the developed electrolytes have a high scattering ability, which makes it possible to plate protective coatings on profile composite units.

The study was carried out using resources of the Center for Collective Use of Scientific Equipment of the Ivanovo State University of Chemistry and Technology.

This work was carried out at the Research Institute of Thermodynamics and Kinetics of Chemical Processes of the Ivanovo State University of Chemistry and Technology and financially supported by the Ministry of Science and Higher Education of the Russian Federation in the framework of the state assignment No. FZZW-2020-0009.

References

1. V. V. Okulov, *Tsinkovanie. Tekhnika i tekhnologiya* [*Zinc-Plating. Technics and Technology*], Globus, Moscow, 2008, 252 pp. (in Russian).
2. M. Schlesinger, M. Paunovic, *Modern Electroplating*, John Wiley & Sons, Hoboken, 2010.
3. E. G. Vinokurov, V. V. Bondar´, *Model´nye predstavleniya dlya opisaniya i prognozirovaniya elektroosazhdeniya splavov* [*Model Concepts for Description and Prediction of Electroplating of Alloys*], VINITI RAN, Moscow, 2009, 164 pp. (in Russian).
4. O. A. Taranina, N. V. Evreinova, I. A. Shoshina, V. N. Naraev, K. I. Tikhonov, *Russ. J. Appl. Chem.*, 2010, **83**, 58.
5. M. H. Gharahcheshmeh, M. H. Sohi, *J. Appl. Electrochem.*, 2010, **40**, 1563.
6. M. M. Kamel, Z. M. Anwer, I. T. Abdel-Salam, I. S. Ibrahim, *Trans. IMF*, 2010, **88**, 191.
7. J. L. Ortiz-Aparicio, Y. Meas, G. Trejo, R. Ortega, T. W. Chapman, E. Chainet, P. Ozil, *J. Appl. Electrochem.*, 2011, **41**, 669.
8. U. Lacnjevac, B. M. Jovic, V. D. Jovic, *J. Electrochem. Soc.*, 2012, **159**, D310.
9. A. V. Krasikov, V. L. Krasikov, *Russ. J. Appl. Chem.*, 2012, **85**, 736.
10. O. Hammami, L. Dhouibi, P. Bercot, E. A. Rezrazi, *Can. J. Chem. Eng.*, 2013, **91**, 19.
11. N. V. Sotskaya, L. V. Sapronova, O. V. Dolgikh, *Russ. J. Electrochem.*, 2014, **50**, 1137.
12. R. Vidu, M. Perez-Page, D. V. Quach, X. Y. Chen, P. Stroeve, *Electroanalysis*, 2015, **27**, 2845.
13. A. Kahoul, F. Azizi, M. Bouaoud, *Trans. IMF*, 2017, **95**, 106.
14. R. F. Shekhanov, S. N. Gridchin, A. V. Balmasov, *Prot. Met. Phys. Chem. Surf.*, 2017, **53**, 483.
15. R. F. Shekhanov, S. N. Gridchin, A. V. Balmasov, *Russ. J. Electrochem.*, 2018, **54**, 355.
16. R. F. Shekhanov, S. N. Gridchin, A. V. Balmasov, *Surf. Eng. Appl. Electrochem.*, 2016, **52**, 152.
17. R. F. Shekhanov, S. M. Kuz´min, A. V. Balmasov, S. N. Gridchin, *Russ. J. Electrochem.*, 2017, **53**, 1274.
18. S. N. Gridchin, R. F. Shekhanov, *Russ. J. Appl. Chem.*, 2019, **92**, 1244.
19. N. G. Bakhchisaraits´yan, Yu. V. Borisoglebskii, G. K. Burkat, *Praktikum po prikladnoi elektrokhimii* [*Practical Works on Applied Electrochemistry*], Khimiya, Leningrad, 1990, 304 pp. (in Russian).
20. I. L. Rozenfeld, *Korroziya i zashchita metallov* [*Corrosion and Protection of Metals*], Metallurgiya, Moscow, 1969, 448 pp. (in Russian).
21. A. A. Bugaevskii, B. A. Dunai, *Zh. Analit. Khim.* [*Sov. J. Anal. Chem.*], 1971, **26**, 205 (in Russian)..
22. V. P. Vasil´ev, V. A. Borosin, E. V. Kozlovskii, *Primenenie EVM v khimiko-analiticheskikh raschetakh* [*Application of Computers in Chemical Analyitcal Calculations*], Vysshaya Shkola, Moscow, 1993, 112 pp. (in Russian).
23. Yu. Yu. Lur´e, *Spravochnik po analiticheskoi khimii* [*Reference Book on Analytical Chemistry*], Al´yans, Moscow, 2013, 448 pp. (in Russian).
24. R. F. Shekhanov, S. N. Gridchin, A. V. Balmasov, *Izv. Vuzov. Khim. Khim. Tekhnol.* [*Bulletin of Higher Educational Institutions. Chem. Chem. Technol.*], 2015, **58**, No. 11, 54 (in Russian).

Received October 1, 2019;
in revised form January 20, 2020;
accepted February 3, 2020